Eur. J. Biochem. 121, 221–232 (1981)


# Conformational Analysis of Peptide Substrates and Inhibitors of the $Zn^{2+}$ G and Serine R61 D-Alanyl-D-alanine Peptidases

Jean-Louis DE COEN, Josette LAMOTTE-BRASSEUR, Jean-Marie GHUYSEN, Jean-Marie FRÈRE, and Harold R. PERKINS

Laboratoire de Chimie biologique, Université Libre de Bruxelles,
Laboratoire de Cristallographie, Université de Liège, Institut de Physique,
Service de Microbiologie, Université de Liège, and
Department of Microbiology, The University of Liverpool

(Received June 16/September 8, 1981)

The tripeptide $N^{\alpha},N^{\varepsilon}$-diacetyl-L-lysyl-D-alanyl-D-alanine ($Ac_2$-LLys$^1$-DAla$^2$-DAla$^3$), which is the standard substrate of the $Zn^{2+}$G and serine R61 D-alanyl-D-alanine peptidases, and several LDD tripeptide analogues where the size and/or the electrical charge of the side chains at position 1, 2 or 3 have been modified (alterations affecting more than one position at the same time were not investigated) have been submitted to conformational analyses based on both short-range and long-range interactions. Among the many backbone conformers of minimal energy of the $\phi_i\psi_i$ space that have been characterized, four types of conformers are the most probable ones. Depending on the peptides, these conformers may have varying relative probability $P$ values so that the leader conformer is not always the same, but, in all cases, the sum of their $P$ values is 90% or more. With the Gly$^1$, Gly$^2$ or Gly$^3$ analogues (which encompass a larger conformational space), the above $\Sigma P$ values are still as high as 35–50%. All the above tripeptides bind to the serine D-alanyl-D-alanine peptidase and with the exception of the Gly$^3$ and Gly$^2$ analogues, to the $Zn^{2+}$ D-alanyl-D-alanine peptidase with virtually the same efficacy, at least within a range of variation of the $K_m$ values for the substrates or the $K_i$ values for the inhibitors, which is less than one order of magnitude. Structural variations at position 1, 2 or 3 in the peptides that are compatible with efficient binding are not necessarily compatible with substrate activity, thus converting the modified peptides into competitive inhibitors. In particular, substrate activity requires a long side chain at position 1 in the peptides. Conformational analyses of $Ac_2$-LLys-DAla-DAla show that the main backbone has a tendency to adopt a ring-like shape from which the LLys side chain protrudes as an extended structure. This latter structure forms with the C-terminal D-alanyl-D-alanine an angle varying between 120° and 180° (depending on the conformers) so that its N-terminal acetyl group is about 1–1.5 nm apart from the scissile amide bond. High turnover numbers (at enzyme saturation) also require a DAla at position 2 with both D-alanyl-D-alanine peptidases and at position 3 in the case of the serine D-alanyl-D-alanine peptidase. Finally, all the conformers of the LAla$^2$ and LAla$^3$ analogues of $Ac_2$-LLys-DAla-DAla fall outside the backbone conformational space that comprises the $\phi_i\psi_i$ angles exhibited by the four types of conformers of the LDD tripeptides. The LAla$^2$ and LAla$^3$ tripeptide analogues do not bind to the serine D-alanyl-D-alanine peptidase (at least at a 10 mM concentration) but they behave as noncompetitive inhibitors of the $Zn^{2+}$ D-alanyl-D-alanine peptidase.

The 18000-$M_r$ G (from *Streptomyces albus* G [1]), the 38000-$M_r$ R61 (from *Streptomyces* R61 [2]) and the 53000-$M_r$ R39 (from *Actinomadura* R39 [3]) D-alanyl-D-alanine peptidases have been used as model enzymes to study the reactions involved in the last step of bacterial wall peptidoglycan synthesis and the mode of action of the $\beta$-lactam antibiotics [4,5]. The G enzyme is a metallo ($Zn^{2+}$) peptidase [6,7]; it functions only as a hydrolase and is highly resistant to penicillin. The R61 and R39 enzymes are serine peptidases [8,9]; they catalyse concomitant hydrolysis and transpeptidation reactions and are moderately and extremely sensitive to penicillin, respectively. In spite of these differences, an examination of the kinetic parameters of the reactions involving a series of peptide analogues [standard reactions: $Ac_2$-LLys$^1$-DAla$^2$-DAla$^3$ + $H_2O$ → $Ac_2$-LLys$^1$-DAla$^2$ + DAla$^3$] has shown [10–12] that whatever the enzyme, substrate activity requires the occurrence of a long side chain at position 1, strictly depends on a DAla at position 2 and accomodates, although at the expense of the catalytic afficiency, Gly or a D-amino acid other than DAla at position 3. LAla at this C-terminal position abolishes substrate activity. This paper describes a theoretical investigation which was undertaken to: (a) determine the most probable conformation of the standard substrate $Ac_2$-LLys-DAla-DAla; (b) delineate how modifications at position 1, 2 or 3 affect this conformation; and (c) possibly relate the conformational changes thus induced, to the effects exerted on the kinetic parameters of the reactions. This study has been limited to the $Zn^{2+}$ G and serine R61 enzymes for which more complete data are available. Moreover, these two enzymes have been crystallized [13,14] and their X-ray structure analyses at 0.45-nm resolution have been or are close to being completed [7,15].

## MATERIALS AND METHODS

### *Enzymes and Peptides*

Fig. 1 is a schematic representation of the active centres of the $Zn^{2+}$ and serine D-alanyl-D-alanine peptidases showing the interactions between the side chains at positions 1, 2 and 3 of $Ac_2$-LLys-DAla-DAla and the corresponding pockets in the enzyme cavity. These interactions permit positioning of

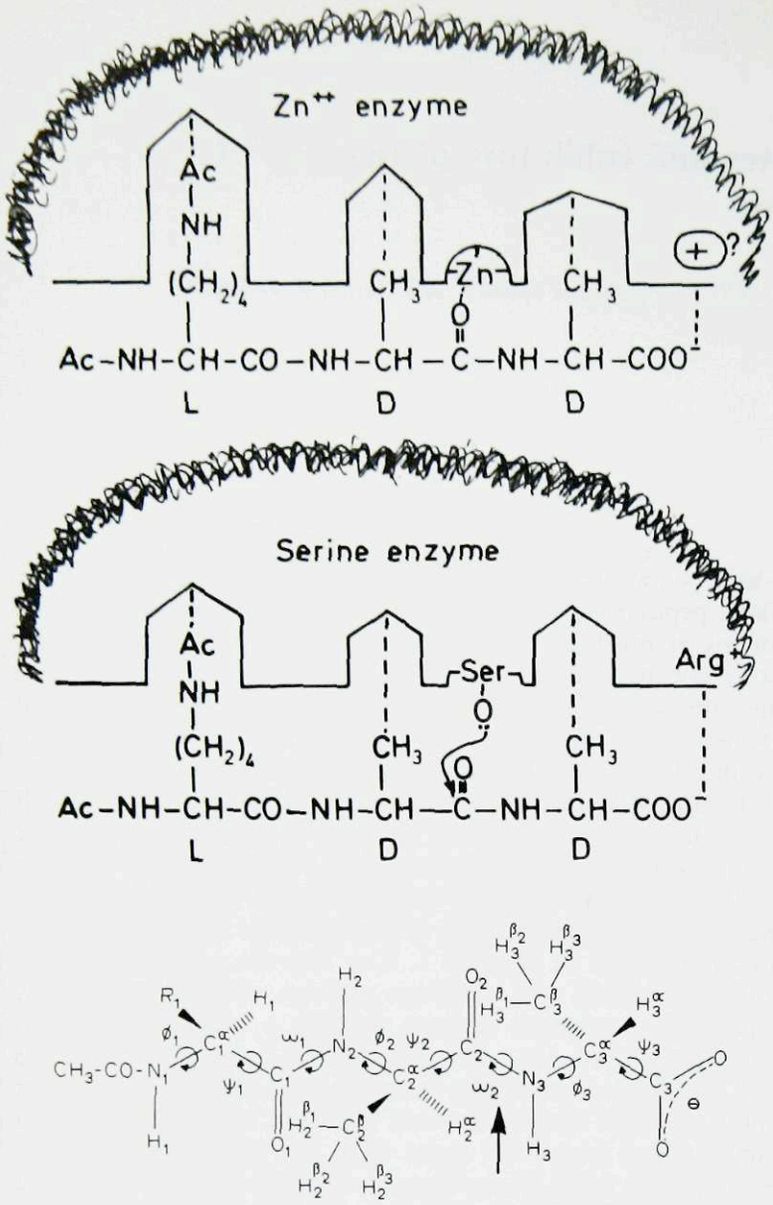


Fig. 1. *Schematic representation of Ac₂-LLys-DAla-DAla bound to the active centres of the $Zn^{2+}$ G and serine R61 D-alanyl-D-alanine peptidases.* In common with carboxypeptidase A and other enzymes acting on anionic substrates, the R61 enzyme possesses an active-site arginine residue [16]. The dihedral angles $\phi_i, \psi_i, \omega_i$ which govern the backbone conformation of the tripeptide $Ac_2$-LLys-DAla-DAla ($R_1$ = the $N^{\epsilon}$-acetylated side chain of LLys) are shown in the lower part of the figure. The arrow indicates the scissile bond

the carbonyl carbon of the sensitive amide bond of the peptide in the vicinity of the $Zn^{2+}$ ion in the G enzyme or the correct serine residue in the R61 enzyme and result in the establishment of the correct active-centre geometry. It has been proposed [4] that initial binding of the peptide to the enzymes mainly depends on the residues at positions 2 and 3 (the sequence DAla-DAla being favorable but not the only efficient one) and that further processing of the Michaelis complex mainly results from a specific interaction between the side chain at position 1 in the bound peptide and an activation site of the enzyme cavity.

The peptides used are listed in Table 1. Some of them are substrates and others are inhibitors. With peptide substrates (S), the maximal velocity $V$ of the reactions has been expressed in turnover number (in $s^{-1}$) and substrate activity has been expressed in terms of $K_m$ and catalytic efficiency, where catalytic efficiency = turnover number/$K_m$. The turnover numbers of the G and R61 enzymes on $Ac_2$-LLys-DAla-DAla are 2.5 $s^{-1}$ and 55 $s^{-1}$, respectively. With the serine R61 enzyme, formation of the Michaelis complex ($E + S \underset{k_{-1}}{\overset{k_1}{\rightleftharpoons}} E \cdot S$ with $k_{-1}/k_1$ = dissociation constant $K$) is thought to be a rapid equilibrium process; moreover, experimental data indicate that the rate of formation of the ester-linked acyl-enzyme intermediate is probably smaller than the rate of enzyme deacylation (R. R. Yocum and J. L. Strominger, personal communication). Consequently, $K_m$ is a valid measure of $K$, the lower the $K_m$ value the more efficient the initial binding of the peptide to the enzyme. The exact mechanistic properties of the $Zn^{2+}$ G enzyme are unkown and therefore $K_m = K$ (also used in the present work) must be regarded as a first approximation.

Non-substrate peptide inhibitors (I) (catalytic efficiency = 0) are peptides which inhibit the hydrolysis of the standard substrate $Ac_2$-LLys-DAla-DAla by the $Zn^{2+}$ or serine D-alanyl-D-alanine peptidase. Double-reciprocal plots of $1/v$ vs $1/[Ac_2\text{-LLys-DAla-DAla}]$ for various [I] values have been used to establish whether the inhibition was competitive (C) or non-competitive (NC); for more details, see legend of Table 1.

The efficacy of the binding process ($E + I \underset{k_{-1}}{\overset{k_{+1}}{\rightleftharpoons}} E \cdot I$) has been expressed as the $K_i$ term, the lower the $K_i$ value the more efficient the binding.

## CONFORMATIONAL ENERGY

The conformational energy $E^{tot}$ is the sum of two terms [19, 20]

$$E^{tot} = E^{loc} + E^{int}. \tag{1}$$

$E^{tot}$ has been estimated using potential functions describing torsional, van der Waals, electrostatic and hydrogen bond energy. $E^{loc}$ (calculated using a grid of 20° for the $\phi, \psi$ angles and 30° for the $\{\chi\}$ angles) defines the conformation of an $n$-peptide (i.e. containing $n$ residues) on the basis of only the local interactions which occur between the atoms surrounding each residue (short-range interactions), thus ignoring the interactions between the various residues:

$$E^{loc} = \sum_{i=1}^{n} E_i^{loc}(\phi_i, \psi_i, \{\chi_i^j\}) \tag{2}$$

where $\{\chi_i^j\}$ stands for $\chi_i^1, \chi_i^2, \chi_i^3, \ldots$ In turn, $E^{int}$ relates to non-local, backbone to backbone, side-chain to backbone and side-chain to side-chain intercations (long-range interactions).

### *Short-Range Interactions*

The probability $P_i^0(\phi_i, \psi_i, \{\chi_i^j\})$ that any residue $i$ of an $n$-peptide assumes given $\phi_i$, $\psi_i$ and $\{\chi_i^j\}$ angle values is estimated according to a Boltzmann distribution

$$P_i^0(\phi_i, \psi_i, \{\chi_i^j\}) = \frac{\exp[-E_i^{loc}(\phi_i, \psi_i, \{\chi_i^j\})/RT]}{\sum_{(\phi_i, \psi_i, \{\chi_i^j\})} \exp[-E_i^{loc}(\phi_i, \psi_i, \{\chi_i^j\})/RT}} \tag{3}$$

where $R$ = gas constant and $T$ = absolute temperature. Summation of the $P_i^0(\phi_i, \psi_i, \{\chi_i^j\})$ values obtained for each set of $\chi_i^j$ angles gives the probability $P_i^0(\phi_i, \psi_i)$ that residue $i$ assumes a given pair of $\phi_i, \psi_i$ angles:

$$P_i^0(\phi_i, \psi_i) = \sum_{\{\chi\}} P_i^0(\phi_i, \psi_i, \{\chi_i^j\}). \tag{4}$$

Table 1. *Efficacy of hydrolysis of peptide substrates by* D-*alanyl-*D-*alanyl peptidase*
The release of the C-terminal residue was measured. Catalytic efficiency = turnover number/$K_m$. NCI = noncompetitive inhibitor; CI = competitive inhibitor. For conditions of synthesis and characterization of the peptides, see [1–3, 10–12]. Data in the table are recalculated from [1–3, 10–12] except for the following. For the noncompetitive inhibitor peptides 2 and 3, the G enzyme (70 ng) and $Ac_2$-LLys-DAla-DAla (at concentrations ranging over 0.37–1.5 mM) were incubated together (at 37 °C and in a total volume of 45 µl of 10 mM Tris/HCl buffer pH 7.8 containing 3 mM $MgCl_2$) in the absence and in the presence of various concentrations of either peptide 2 or peptide 3 (at concentrations ranging up to 0.9 mM). The released D-alanine (in low amounts down to 1 nmol) was estimated according to the method of Martin et al. [17] modified as follows. The reaction mixtures were successively heated at 100 °C for 1 min, cooled to 37 °C, supplemented with a solution (60 µl) of D-amino acid oxidase (1 µg) and FAD (3 µg) made in 100 mM Tris/HCl buffer pH 8.0, cooled to 18 °C, supplemented with a solution (20 µl) of horse radish peroxidase (0.65 µg) and ABTS dye (35 µg; from Boehringer) made in water, and further incubated at 18 °C for 5 min. After addition of 250 µl water, the absorbance of the solutions was measured at 410 nm; 1 nmol of D-alanine produces an absorbance of 0.10. The results were analysed using the least-square program of Schilf et al. [18]. The values of the Fischer-Snedecor variables $F$ were highly significant of a noncompetitive model ($F_{meas.} > F_{99}$). For $K_i$ and $K_i'$ values, see text. For peptide 4, assuming a competitive inhibition, the $K_i$ values were determined under the following conditions of substrate and inhibitor concentrations: 0.8 mM $Ac_2$-LLys-DAla-DAla and 0–2 mM inhibitor in the case of the G enzyme; 7 mM $Ac_2$-LLys-DAla-DAla and 0–8 mM inhibitor in the case of the R61 enzyme. For the competitive inhibitor peptide 5, the $K_i$ values were determined under the following conditions of substrate and inhibitor concentrations: 0.7–3 mM $Ac_2$-LLys-DAla-DAla and 0–1.5 mM inhibitor in the case of the G enzyme; 1.5–7 mM $Ac_2$-LLys-DAla-DAla and 0–8.5 mM inhibitor in the case of the R61 enzyme. For peptide 14, the $K_i$ values were computed from [12] assuming a competitive inhibition. For peptide 15, the $K_i$ values were computed from [12]. The inhibition of the G enzyme by Ac-DAla-DGlu was shown to be competitive [12]. That the inhibition of the R61 enzyme is also competitive is supported by the fact that the close analogue Ac-DAla-DAsp which is a better inhibitor ($K_i \approx 4$ mM) behaves this way [12]. n.d. = not determined

| Peptides | 18000-$M_r$ G enzyme | | 38000-$M_r$ R61 enzyme | |
|---|---|---|---|---|
| | $K_m$ (for substrate) and $K_i$ (for inhibitor) | catalytic efficiency | $K_m$ (for substrate) and $K_i$ (for inhibitor) | catalytic efficiency |
| | mM | $M^{-1}\,s^{-1}$ | mM | $M^{-1}\,s^{-1}$ |
| 1. $Ac_2$-LLys-DAla-DAla | 0.33 | 7600 | 12 | 4600 |
| 2. $Ac_2$-LLys-LAla-DAla | (NCI) | 0 | (no binding at 10 mM) | 0 |
| 3. $Ac_2$-LLys-DAla-LAla | (NCI) | 0 | (no binding at 10 mM) | 0 |
| 4. $Ac_2$-LLys-DLeu-DAla | 0.8 | 0 | 10 | 60 |
| 5. $Ac_2$-LLys-DGlu-DAla | 0.70 (CI) | 0 | 10 (CI) | 0 |
| 6. $Ac_2$-LLys-DAla-DLeu | 0.33 | 2500 | 10 | 310 |
| 7. $Ac_2$-LLys-DAla-DLys | 0.80 | 2700 | 13 | 430 |
| 8. $Ac_2$-LLys-Gly-DAla | 15 | 180 | 15 | 7 |
| 9. $Ac_2$-LLys-DAla-Gly | 2.50 | 600 | 36 | 350 |
| 10. $Ac_2$-L$A_2$bu-DAla-DAla | 0.6 | 1300 | (8 %)[b] | |
| 11. UDP-MurNAc-Gly-DGlu[LHse-DAla-DAla][a] | 1.0 | 300 | (3 %)[b] | |
| 12. Ac-LAla-DAla-DAla | 3.3 | 3 | (1.4 %)[b] | |
| 13. Ac-Gly-DAla-DAla | 1.1 | 30 | n.d. | |
| 14. Ac-DAla-DAla | 20 | 0 | 230 | 0 |
| 15. Ac-DAla-DGlu | 0.2 (CI) | 0 | 25 (CI) | 0 |

[a] Uridine-diphospho-*N*-acetylmuramyl-glycyl-D-γ-glutamyl-L-homoseryl-D-alanyl-D-alanine.

[b] Substrate activity determined at 0.5 mM and expressed relatively to that of $Ac_2$-LLys-DAla-DAla (100 %) tested under identical conditions; see [10–12].

Plotting the $P_i^0(\phi_i, \psi_i)$ values on a classical Ramachandran's $\phi,\psi$ map [21] permits visualization of regions $R$ of various probabilities. Fig. 2 shows the $P^0(\phi_i, \psi_i)$ map of an LAla dipeptide unit; the regions of high probability are designated by capital letters A, B, C, D, E ... and A*, B*, C*, D*, E* ... (for the two symmetrical regions in the $\phi,\psi$ space, respectively). Region A corresponds to the well-known right-handed α-helix; region B includes the $\phi,\psi$ angles characteristic of the β-pleated sheets. In turn, Fig. 3 shows the $P^0(\phi,\psi)$ maps of an LAla unit in a C-terminal position.

*Long-Range Interactions*

When the $E^{int}$ term of Eqn (1) is taken into account, the probability $P([\phi_i, \psi_i, \{\chi_i^j\}])$ that an $n$-peptide adopts a given set of $[\phi_i, \psi_i, \{\chi_i^j\}]$ values is given by

$$P([\phi_i,\psi_i,\{\chi_i^j\}]) = \frac{\exp[-E^{tot}([\phi_i,\psi_i,\{\chi_i^j\}])/RT]}{\sum_{(\phi_i,\psi_i,\{\chi_i^j\})} \exp[-E^{tot}([\phi_i,\psi_i,\{\chi_i^j\}])/RT]}. \quad (5)$$

## RESULTS

*Conformational Analysis*

Ramachandran's maps like those shown in Fig. 2 and 3 (see Materials and Methods; short-range interactions) can be used to evaluate three types of probability $P^0$. (a) Summation of all the individual $P_i^0(\phi_i, \psi_i)$ values [Eqn (4)] which are comprised in a given region $R$, gives the probability, $P_i^0(R_i)$, according to which residue $i$ occupies this particular region. (b) On the basis of these individual $P_i^0(R_i)$ values, the probability $P^0(R_1, R_2 \ldots R_n)$ that an $n$-peptide assumes a given family $R_1, R_2 \ldots R_n$ of backbone conformations is given by

$$P^0(R_1, R_2 \ldots R_n) = P^0(R_1) \times P^0(R_2) \times \ldots \times P^0(R_n).$$

(c) If the points within the various regions $R$ are represented by the corresponding small letters $r$, the probability $P^0(r_1, r_2 \ldots r_n)$ which characterizes one conformer $r_1, r_2 \ldots r_n$ of a given family $R_1, R_2 \ldots R_n$ is given by

$$P^0(r_1, r_2 \ldots r_n) = P^0(r_1) \times P^0(r_2) \times \ldots \times P^0(r_n).$$

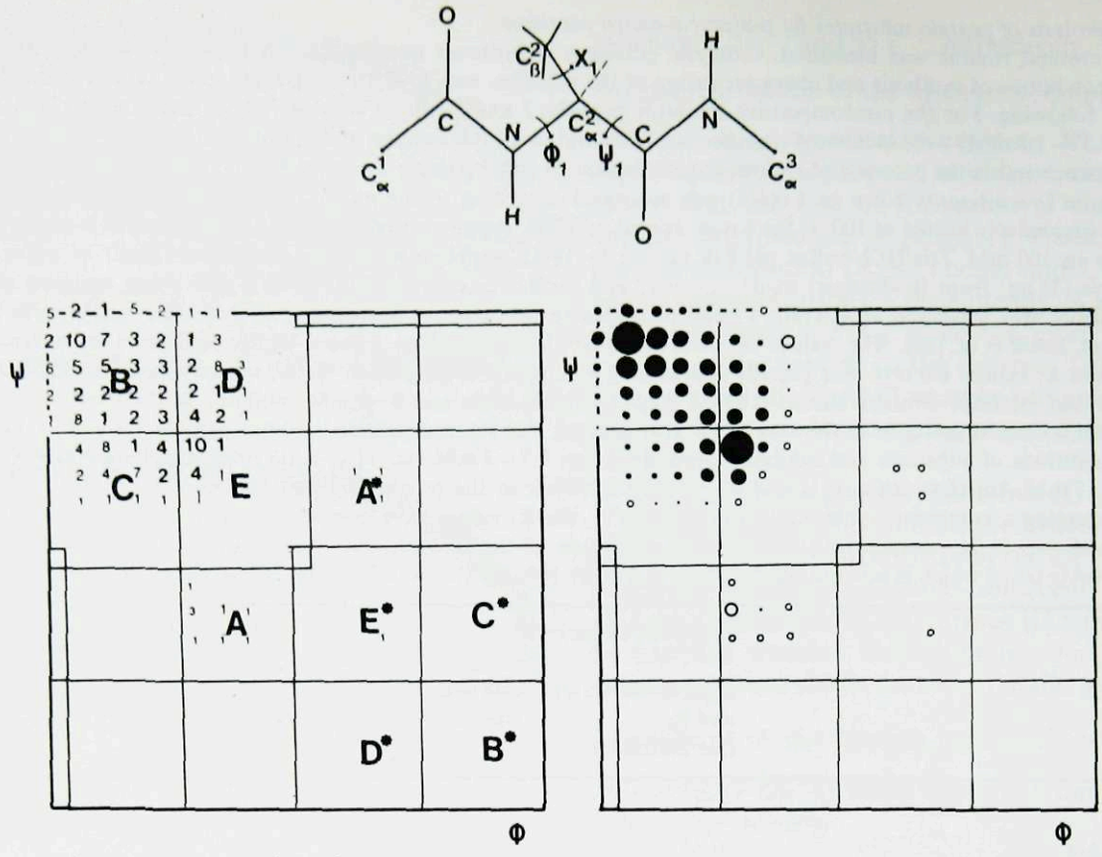


Fig. 2. *Probability map* $P^0$ $(\phi,\psi)$ *of the* $C\alpha^1 - C\alpha^3$ *segment of a polypeptide chain with an* LAla *residue at position 2 (*LAla *dipeptide unit).* Left: probability map $P^0$ $(\phi,\psi)$ where capital, medium and small numbers give $P^0$ in $^0/_0$, $^0/_{00}$ and $^0/_{000}$, respectively. The regions of high probability are labelled with capital letters A, B, C, D, E and A*, B*, C*, D*, E* for the symmetrical ones. Right: schematic probability map $P^0$ $(\phi,\psi)$ of the same LAla dipeptide unit. The area of the black or white disks are respectively proportional to $P^0$ and $10^{-1}$ $P^0$

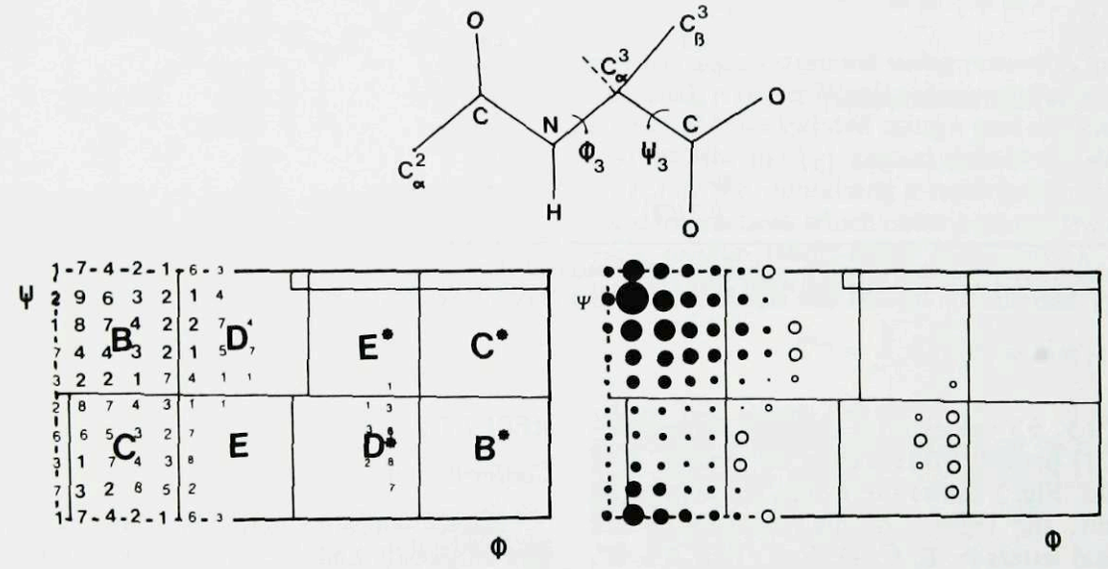


Fig. 3. *Probability map* $P^0$ $(\phi,\psi)$ *of an* LAla *unit at the C-terminal position.* $\psi_3$ values between 0° and −180° (not shown) are equivalent to $\psi_3$ values between 180° and 0°

The above approach has been applied to the standard tripeptide $Ac_2$-LLys-DAla-DAla and the peptide analogues listed in Table 1. The summation on the $\chi$ angles [Eqn (4)] has been restricted to those positions of the side chains for which the corresponding local energy levels do not exceed the optimal value by 21 kJ. The following observations have been made. (a) The probability distributions $P_i^0(\phi_i,\psi_i)$ (calculated at 298 K) of the various residues which constitute the peptides under consideration are shown in Fig. 4 (maps 1 − 15). (b) The probabilities $P_i^0(R_i)$ according to which each residue at position 1, 2 or 3 of the peptides, occupies the various regions $R$ of the Ramachandran's maps are given in Table 2. They have been obtained by summing up the 25 individual $P_i^0(\phi_i,\psi_i)$ values of each of the regions A, B . . ., A*, B* . . . of the maps of Fig. 4. (c) The probability $P^0$ $(R_1, R_2, R_3)$ according to which any of the tripeptides assumes a given family $R_1, R_2, R_3$ of backbone conformations can be calculated from the data of Table 2. With $Ac_2$-LLys-DAla-DAla, family BB*B* has a $P^0$ (B, B*, B*) value of $0.70 \times 0.61 \times 0.79 = 34\%$ and is the most populated one. In turn, the families BE*B*, EB*B*, EE*B*, etc. have $P^0$ values of 8.3 %, 5.3 %, 1.3 %, etc. (d) Using the points $r$ of maximal $P^0$ values of the $(\phi_i,\psi_i)$

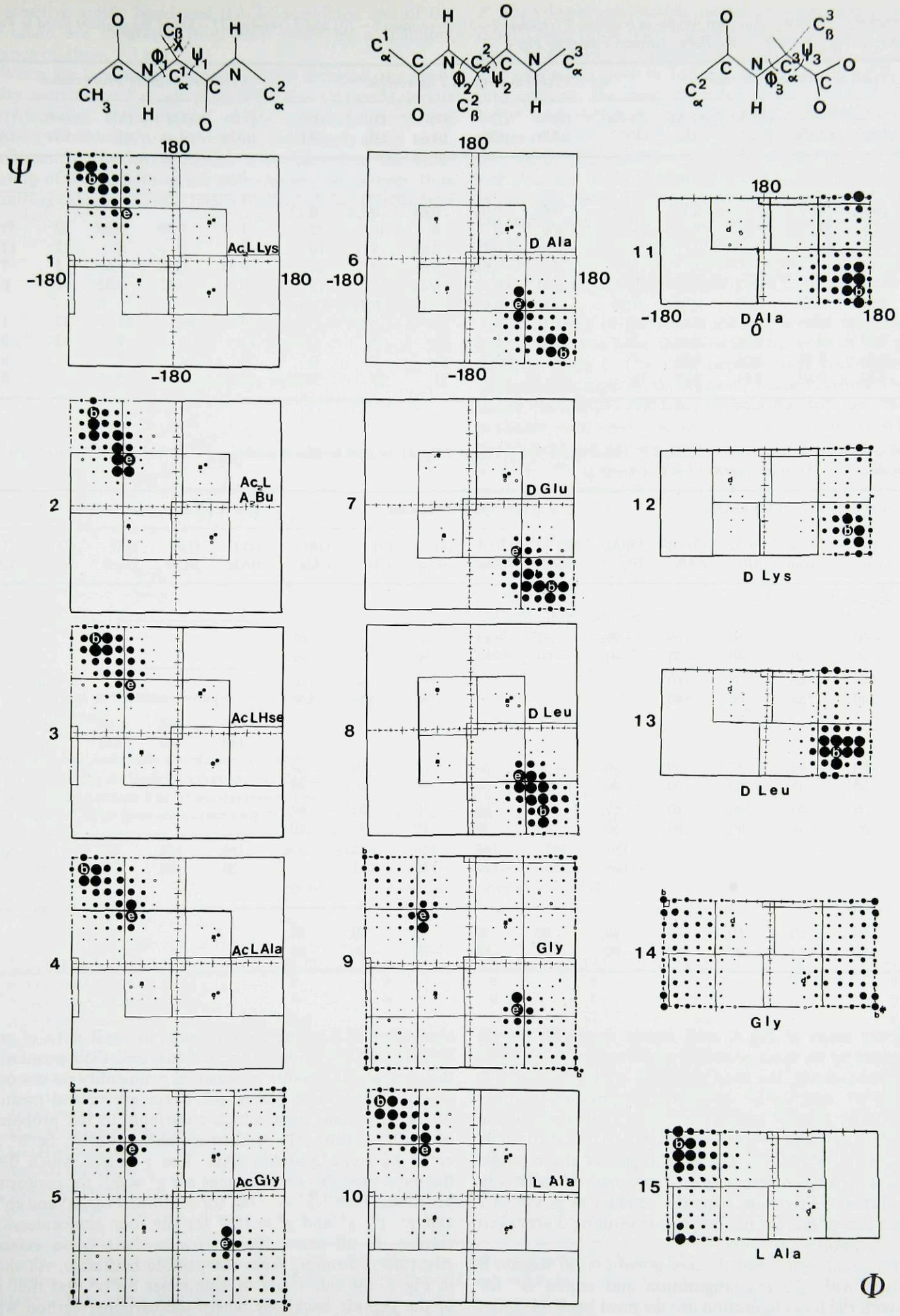


Fig. 4. *Probability maps* $P^0$ *(φ,ψ) for each residue at positions 1 (maps 1–5), 2 (maps 6–10) and 3 (maps 11–15) of the peptides listed in Table 1.* Points of maximal probability in regions A, B, E, A*, B*, E*, are identified by small letters a, b, e, a*, b*, e*

Table 2. *Probability* $P_i^0$ ($R_i$) *that each residue at positions 1 (residues 1–5), 2 (residues 6–10) and 3 (residues 11–15) of the peptides listed in Table 1 occupies the various regions* R *of the Ramachandran's maps of Fig. 4*

| Region | $P_1^0(R_i)$ at position 1 for residue | | | | | $P_1^0(R_i)$ at position 2 for residue | | | | | $P_1^0(R_i)$ at position 3 for residue | | | | |
|---|---|---|---|---|---|---|---|---|---|---|---|---|---|---|---|
| | (1) Ac$_2$-LLys | (2) Ac$_2$-LA$_2$bu | (3) Ac-LHse | (4) Ac-LAla | (5) Ac-Gly | (6) DAla | (7) DGlu | (8) DLeu | (9) Gly | (10) LAla | (11) DAla | (12) DLys | (13) DLeu | (14) Gly | (15) LAla |
| | % | | | | | | | | | | | | | | |
| A | 0.06 | 0.12 | 0.15 | 0.14 | 0.12 | 0.04 | 0.05 | 0.04 | 0.12 | 0.12 | | | | | |
| B | 70 | 59 | 69 | 59 | 15 | 0 | 0 | 0 | 16 | 61 | 1 | 0.79 | 0.08 | 32 | 79 |
| C | 11 | 16 | 9 | 10 | 7 | 0.01 | 0 | 0.01 | 7 | 10 | 0 | 0 | 0 | 12 | 12 |
| D | 8 | 9 | 13 | 14 | 7 | 0 | 0.01 | 0.01 | 7 | 14 | 0.34 | 0.36 | 0.66 | 5 | 7 |
| E | 11 | 15 | 9 | 16 | 18 | 0.01 | 0.03 | 0.04 | 17 | 15 | 0.01 | 0.01 | 0.02 | 1 | 0.52 |
| A* | 0.08 | 0.17 | 0.05 | 0.05 | 0.12 | 0.12 | 0.08 | 0.11 | 0.12 | 0.04 | | | | | |
| B* | 0 | 0 | 0 | 0 | 15 | 61 | 70 | 60 | 16 | 0 | 79 | 86 | 82 | 32 | 1 |
| C* | 0.01 | 0 | 0.01 | 0.01 | 7 | 10 | 6 | 13 | 7 | 0.01 | 12 | 8 | 9 | 12 | 0 |
| D* | 0.01 | 0.01 | 0.01 | 0.01 | 7 | 14 | 17 | 16 | 7 | 0 | 7 | 4 | 7 | 5 | 0.34 |
| E* | 0.02 | 0.04 | 0.01 | 0.01 | 18 | 15 | 6 | 11 | 17 | 0.01 | 0.52 | 0.14 | 0.46 | 1 | 0.01 |

Table 3. $\phi,\psi$ *angles at those points of maximal* $P^0$ *values of the* $(\phi_i,\psi_i)$ *space (Fig. 4) for each residue at positions 1 (residues 1–5), 2 (residues 6–10) and 3 (residues 11–15) of the peptides listed in Table 1*

| Point of maximal $P^0$ | $\phi,\psi$ at position 1 for residue | | | | | $\phi,\psi$ at position 2 for residue | | | | | $\phi,\psi$ at position 3 for residue | | | | |
|---|---|---|---|---|---|---|---|---|---|---|---|---|---|---|---|
| | (1) Ac$_2$-LLys | (2) Ac$_2$-LA$_2$bu | (3) Ac-LHse | (4) Ac-LAla | (5) Ac-Gly | (6) DAla | (7) DGlu | (8) DLeu | (9) Gly | (10) LAla | (11) DAla | (12) DLys | (13) DLeu | (14) Gly | (15) LAla |
| | degrees | | | | | | | | | | | | | | |
| a | −60, −40 | −80, −40 | −60, −40 | −60, −40 | −60, −60 | −60, −60 | −40, −60 | −60, −60 | −60, −60 | −60, −40 | | | | | |
| b | −140, 140 | −140, 160 | −160, 160 | −180, 180 | | | | −180, 180 | −180, 180 | −160, 160 | | | | −180, 180 | −160, 160 |
| d | | | | | | | | | | | −60, 140 | −60, 140 | −60, 140 | −60, 140 | |
| e | −80, 80 | −80, 80 | −80, 80 | −80, 80 | −80, 80 | −60, 60 | −60, 80 | −60, 60 | −80, 80 | −80, 80 | | | | | |
| a* | 60, 60 | 40, 60 | 40, 60 | 60, 60 | 60, 60 | 60, 40 | 60, 40 | 60, 40 | 60, 60 | 60, 60 | | | | | |
| b* | | | | | 180, −180 | 160, −160 | 140, −140 | 120, −140 | 180, −180 | | 160, 20 | 140, 40 | 120, 40 | 180, 0 | |
| d* | | | | | | | | | | | | | | 60, 40 | 60, 40 |
| e* | 60, −60 | 60, −60 | 60, −60 | 60, −60 | 80, −80 | 80, −80 | 80, −80 | 80, −80 | 80, −80 | 60, −60 | | | | | |

space of the maps of Fig. 4, each family $R_1, R_2, R_3$ can be characterized by its most probable conformer $r_1, r_2, r_3$. With Ac$_2$-LLys-DAla-DAla, the most probable conformers bb*b*, be*b*, eb*b* and ee*b* of the corresponding families BB*B*, BE*B*, EB*B* and EE*B*, have approximately the same 0.072% absolute $P^0$ probability (i.e. $0.08 \times 0.10 \times 0.09$ for conformer bb*b*). (e) The $\phi,\psi$ angles of those points of the $(\phi_i,\psi_i)$ space corresponding to maximal $P^0$ values are given in Table 3. Five points for the residues at positions 1 and 2, and two points for the residues at position 3 are taken into consideration.

The following comments deserve attention. (a) Region B for residues with the L configuration and region B* for residues with the D configuration are the most probable ones. (b) Substitution of one residue at position 1, 2 or 3 of the tripeptide Ac$_2$-LLys-DAla-DAla by another residue exhibiting the same L or D configuration results in small shifts of probability. (c) Depending on the residues and their positions in the peptides, the points of maximal probability do not occur exactly at the same places. (d) There are several positions of the LLys side chain which contribute to the probability of the most probable conformers bb*b*, eb*b*, be*b* and ee*b* of Ac$_2$-LLys-DAla-DAla. The $\chi$ angles which define the most probable arrangement are $\chi^1 = 60°$ for conformers bb*b* and be*b*, $\chi^1 = -60°$ for conformers ee*b* and eb*b*, and $\chi^2$, $\chi^3$, $\chi^4$ and $\chi^5 = 180°$ for the four conformers considered. In all cases, the LLys side chain is an extended structure protruding from the peptide backbone. As shown in Fig. 5, the side chain of conformer bb*b* and that part of the peptide backbone where the carbonyl carbon which undergoes nucleophilic attack is located, form between them an angle of about 120°. Moreover, the carbonyl carbon of

the sensitive amide bond and the $N^{\varepsilon}$-acetylated end of the side chain are separated from each other by a spanning distance of about 1.3 nm.

When the long-range interactions are included, the probability distribution $P$ is calculated from Eqn (5) (see Materials and Methods). Computation of the denominator of this equation would have required an exceedingly long time. Consequently, the investigations were limited to the computation of the numerator for well-selected conformers, thus permitting calculation of a relatively probability distribution

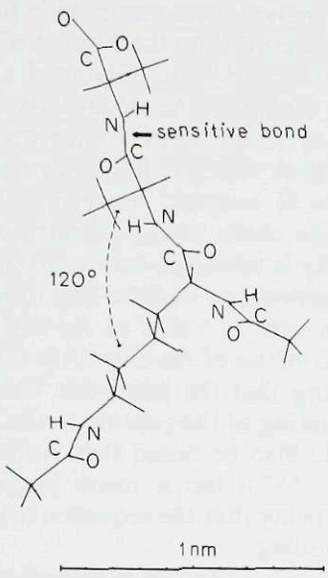


Fig. 5. *Side chain to backbone arrangement found in conformer bb*b* of* $Ac_2$-LLys-DAla-DAla

$P$. The selected conformers, each of them representing a given family, were those corresponding to the points of the $(\phi_i, \psi_i)$ space of maximal $P^0$ values (for the $\phi, \psi$ angles, see Table 3). The results are given in Table 4. Note that when $E^{int}$ is taken into account, the most probable conformers ee*b*, bb*b*, be*b* and eb*b* of $Ac_2$-LLys-DAla-DAla have relative $P$ values of 36.3%, 31.7%, 17.2% and 7.3%, respectively (while they were equiprobable at the $P^0$ level; see above). The relative $P$ values of the dipeptides Ac-DAla-DAla and Ac-DAla-DGlu were similarly estimated; conformers b*b* and e*b* are largely predominant (Table 4). The whole conformational space of Ac-DAla-DAla was scanned and the denominator of Eqn (5) computed. The results were that families B*B* and E*B* also largely predominate (34.2% and 16.2%, respectively).

As a result of the above studies, several backbone conformations have been characterized for each of the peptides listed in Table 1. For each peptide, that conformer which characterizes itself by the highest $P$ value is referred to as the leader conformer. The leader conformer and the other most probable conformers which have been used to define the conformational characteristics of a given peptide represent at least 90% of all the conformers taken into account ($\Sigma P_{relative}$ values > 90%; see Table 4).

## RELATIONSHIPS BETWEEN CONFORMATION AND SUBSTRATE OR INHIBITOR ACTIVITY

$Ac_2$-LLys-DAla-DAla is the peptide which exhibits the highest substrate activity with the G and R61 D-alanyl-D-alanine peptidases (Table 1). Fig. 6a–d are stereoscopic views of the leader conformer ee*b* and the three other most probable conformers bb*b*, be*b* and eb*b* ($\Sigma P_{relative}$ values = 93%). The $N^{\alpha}$ and $N^{\varepsilon}$-acetyl groups are situated at the right and left sides, respectively, of the lower part of the

Table 4. *Relative probability distribution of conformers at the* P *level*

The predominating or leader conformers are printed in bold-face type. Note that when Gly occurs at position 1, 2 or 3 (peptides 13, 8 and 9), the corresponding points b or b* are equivalent (see maps 5, 9 and 14 in Fig. 4). Also that when LAla occurs at position 2 or 3 (peptides 2 and 3), the points b and b* differ from each other only by +40° or −40° for both $\phi\psi$ angles (see maps 6 and 10, 11 and 15 in Fig. 4)

| Peptide | $P$ for conformer | | | | | | |
|---|---|---|---|---|---|---|---|
| | bb*b* | eb*b* | e*b*b* | be*b* | ee*b* | e*e*b* | $\Sigma$ |
| | % | | | | | | |
| 1. $Ac_2$-LLys-DAla-DAla | 31.75 | 7.3 | 0 | 17.2 | **36.3** | 0 | 92.55 |
| 2. $Ac_2$-LLys-LAla-D-Ala[a] | 0 | 0 | 0 | 0 | 0 | 0 | 0 |
| 3. $Ac_2$-LLys-DAla-LAla[b] | 0 | 0 | 0 | 0 | 0 | 0 | 0 |
| 4. $Ac_2$-LLys-DLeu-DAla | **61.4** | 7 | 0 | 12.7 | 13.4 | 0 | 94.5 |
| 5. $Ac_2$LLys-DGlu-DAla | 31.5 | 6.5 | 0 | **40.8** | 14 | 0 | 92.8 |
| 6. $Ac_2$-LLys-DAla-DLeu | 1.5 | 0.4 | 0 | 9.4 | **85.6** | 0 | 96.9 |
| 7. $Ac_2$-LLys-DAla-DLys | 18.2 | 7.5 | 0 | **50.6** | 13.9 | 1.9 | 92.1 |
| 8. $Ac_2$-LLys-Gly-DAla[c] | 0 | 0 | 0 | 13.5 | 27.8 | 0 | 41.3 |
| 9. $Ac_2$-LLys-DAla-Gly[d] | 17.7 | 0 | 3.9 | 7.2 | 10.9 | 0 | 39.7 |
| 10. $Ac_2$-L$A_2$bu-DAla-DAla | 21.2 | 8.55 | 0 | 23.8 | **37.5** | 0 | 91 |
| 11. Ac-LHse-DAla-DAla | 27.1 | 6.7 | 0 | 23.7 | **33.7** | 0 | 91.2 |
| 12. Ac-LAla-DAla-DAla | 21.3 | 9.3 | 0 | 17.2 | **44** | 0 | 91.8 |
| 13. Ac-Gly-DAla-DAla[e] | 0 | 9.7 | 13.2 | 2.5 | **42.8** | 19.50 | 87.7 |
| 14. Ac-DAla-DAla | | b*b* = **61.8** | | | e*b* = 34.1 | | 95.9 |
| 15. Ac-DAla-DGlu | | b*b* = 41.6 | | | e*b* = **55** | | 96.6 |

[a] beb* = **40.2**; bbb* = 25.2; eeb* = 16.6; ebb* = 9.6; eab* = 2.6; bed = 1.5; ea*b* = 1.4. $\Sigma$ = 97.1

[b] bb*b = **32.1**; ee*b = 24.1; ea*b = 15.2; be*b = 15.1; eb*b = 7.2; bab = 1.8; ba*b = 1.1. $\Sigma$ = 96.6.

[c] beb* = **34.5**; eeb* = 11.2. $\Sigma$ = 87.

[d] ee*d = **31**; bb*d* = 6.3; bb*d = 5.1; be*d = 4.9; ea*e* = 3.3; bad = 1.9. $\Sigma$ = 92.2.

[e] ee*d = 3.5. $\Sigma$ = 91.2

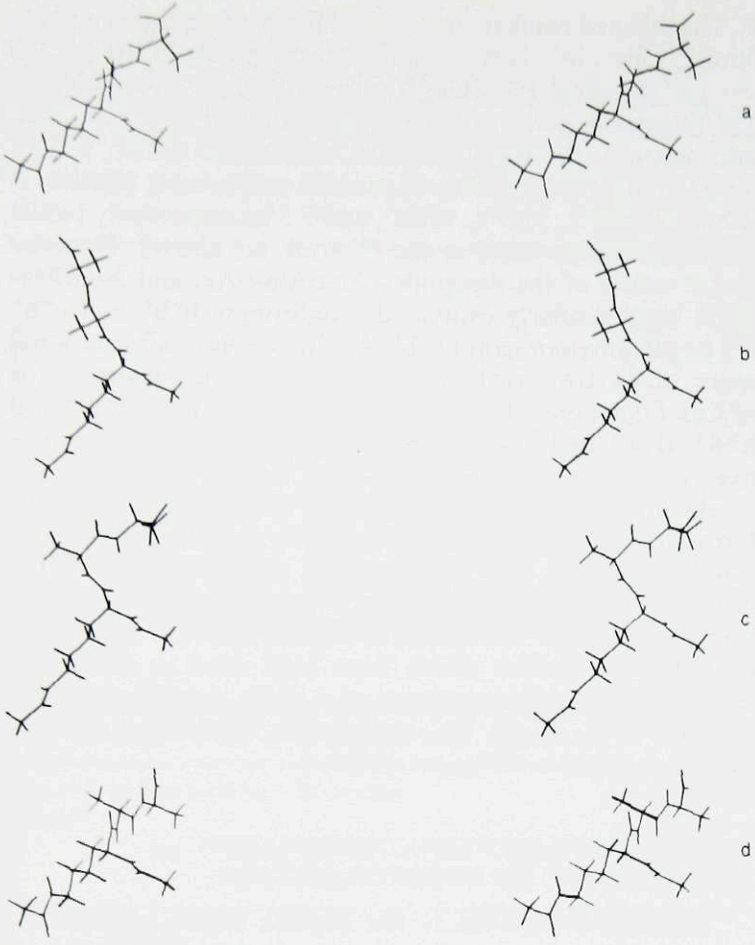


Fig. 6. *Stereoscopic diagrams of the four most probable conformers of* $Ac_2$-LLys-DAla-DAla: *ee*b* (Fig. a), bb*b* (Fig. b), be*b* (Fig. c) and eb*b* (Fig. d).* The leader conformer is ee*b*

figures (the same general orientation is used in Fig. 5). The following observations can be made. (a) Irrespective of the conformer considered, the $N^{\varepsilon}$-acetylated side chain of the LLys residue ($R_1$) is an extended structure which protrudes from the main peptide backbone:

$$\begin{array}{l} \qquad\quad R_1 \qquad\quad CH_3 \qquad\quad CH_3 \\ CH_3\text{–}CONH\text{–}CH\text{–}CONH\text{–}CH\text{–}CONH\text{–}CH\text{–}CONH. \\ \qquad\quad (L) \qquad\quad (D) \qquad\quad (D) \end{array}$$

(b) The $N^{\varepsilon}$-acetylated side chain and the C-terminal DAla-DAla portion of the peptide backbone form at the L-centre of the peptide, an angle of 120° in conformers bb*b* and be*b*, and 180° in conformers ee*b* and eb*b*. (c) The C-terminal DAla somewhat folds back towards the $N^{\alpha}$-acetylated terminal group in conformers eb*b*, be*b* and ee*b*, the strongest curvature of the loop being observed in conformer ee*b*. Ring-like structures have also been proposed for the peptide units of the bacterial wall peptidoglycan by Barnickel et al. [22].

In order to determine the relationships which must exist between conformation and substrate activity, four types of structural alterations of $Ac_2$-LLys-DAla-DAla have been investigated and the conformational changes thus induced (Table 4) have been related to the effects exerted on the kinetic parameters of the reactions (Table 1). Note that all the peptides of Table 1 and the corresponding ones of Table 4 are identical except peptide 11 (UDP-MurNAc-Gly-DGlu-[LHse-DAla-DAla] cf. Ac-LHse-DAla-DAla).

*Shortening the Neutral Side Chain at the L-Centre of* $Ac_2$-LLys-DAla-DAla

These alterations (peptides 1 and 10–15 in Tables 1 and 4) give rise only to minor modifications of the equilibrium distribution. The $\Sigma P_{relative}$ (bb*b*, eb*b*, be*b*, ee*b*) values of the $Ac_2$-L$A_2$bu[1], Ac-LHse[1] and Ac-LAla[1] analogues remain higher than 90%. As expected, the Ac-Gly[1] analogue encompasses a larger proportion of the conformational space; however, conformer ee*b* remains the leader, the $\Sigma P_{relative}$ (bb*b*, eb*b*, be*b*, ee*b*) is still 50% and the e*b*-b*b* probability of the C-terminal dipeptide remains close to 90%.

When compared to $Ac_2$-LLys-DAla-DAla, the modified peptides bind somewhat less effectively to the G enzyme, the $K_m$ value being increased at the most by a factor of 3 to 10. The main effect, however, is on the $V$ value which is decreased by a factor of 100–200 for the Gly[1] and LAla[1] analogues. At the limit, the dipeptide Ac-DAla-DAla (b*b* = 61.8%; e*b* = 34.1%) is a nonsubstrate competitive inhibitor.

The data obtained with the R61 enzyme are limited. As observed with the G enzyme, however, substrate activity requires a long side chain at the L-centre of the tripeptide and enzyme activity is inhibited by Ac-DAla-DAla.

Two other observations deserve attention. With both G and R61 enzymes, the $K_i$ value of Ac-DAla-DAla is much higher than the $K_m$ values of Ac-Gly-DAla-DAla or $Ac_2$-LLys-DAla-DAla, showing that the tripeptide backbone is of importance in the binding of the peptide to the $Zn^{2+}$ and serine enzymes. It should also be noted that Ac-DAla-DGlu (b*b* = 41.6%; e*b* = 55%) has a much lower $K_i$ value than Ac-DAla-DAla showing that the sequence DAla-DGlu permits a more efficient binding.

*Replacing DAla by Other D-Amino Acids at Position 2 or 3 of* $Ac_2$-LLys-DAla-DAla

Replacing DAla at position 2 by DLeu or DGlu (peptides 4 and 5 in Tables 1 and 4) considerably enhances the probability of conformers bb*b* and be*b*, respectively, the stabilization effect resulting from the establishment of close contacts between the DLeu or the DGlu side chain and the LLys side chain (Fig. 7a, b). Replacing DAla at position 3 by DLeu or DLys (peptides 6 and 7 in Tables 1 and 4) considerably enhances the probability of conformers ee*b* and be*b*, respectively, the observed conformational shifts resulting from the establishment of good contacts between the DLeu or DLys side chain and the peptide backbone (Fig. 7c, d). All these alterations modify the probability patterns of the four most probable conformers ee*b*, bb*b*, be*b* and eb*b*, but the $\Sigma P_{relative}$ (ee*b*, bb*b*, be*b*, eb*b*) values always remain higher than 90%.

The modified peptides bind to the R61 enzyme with the same efficacy as $Ac_2$-LLys-DAla-DAla but modifications at position 3 (peptides 6 and 7) decrease the $V$ value by a factor of 10 and modifications at position 2 (peptides 4 and 5) abolish substrate activity so that the peptides are converted into nonsubstrate inhibitors. The $K_m$ of $Ac_2$-LLys-DAla-DAla and the $K_i$ of the competitive inhibitor $Ac_2$-LLys-DGlu-DAla are virtually identical.

As observed with the R61 enzyme, binding of the modified peptides to the G enzyme is not or is very little affected and modification at position 2 (peptides 4 and 5) abolish catalysis, converting the peptides into nonsubstrate competitive inhibitors. When compared with $Ac_2$-LLys-DAla-DAla ($K_m$

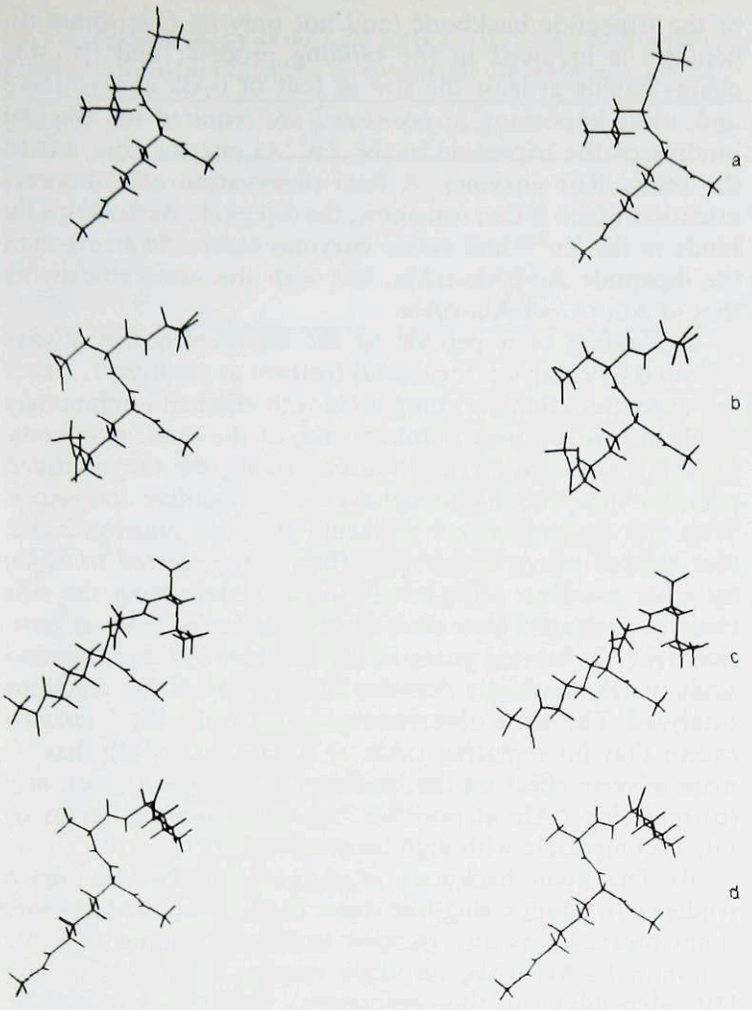


Fig. 7. *Stereoscopic diagrams of the leader conformers of* $Ac_2$-LLys-DLeu-DAla *(bb*b*; Fig. a); Ac*$_2$*-LLys-DGlu-DAla (be*b*; Fig. b); Ac*$_2$*-LLys-DAla-DLeu (ee*b*; Fig. c); Ac*$_2$*-LLys-DAla-DLys (be*b*; Fig. d)*

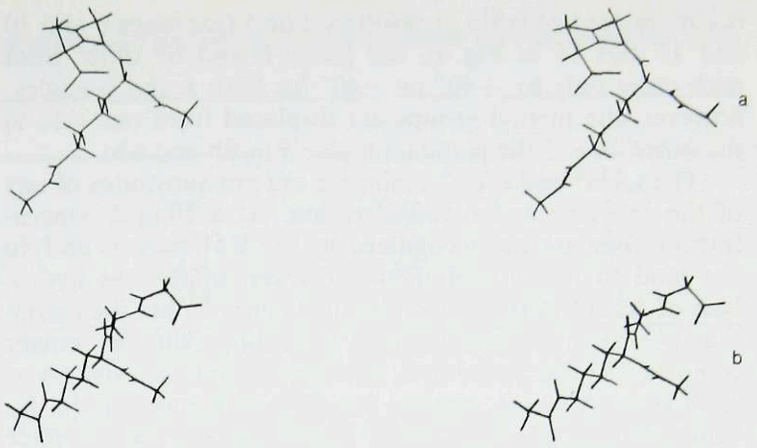


Fig. 8. *Stereoscopic diagrams of the leader conformers of* $Ac_2$-LLys-Gly-DAla *(beb*; Fig. a) and Ac*$_2$*-LLys-DAla-Gly (ee*d; Fig. b)*

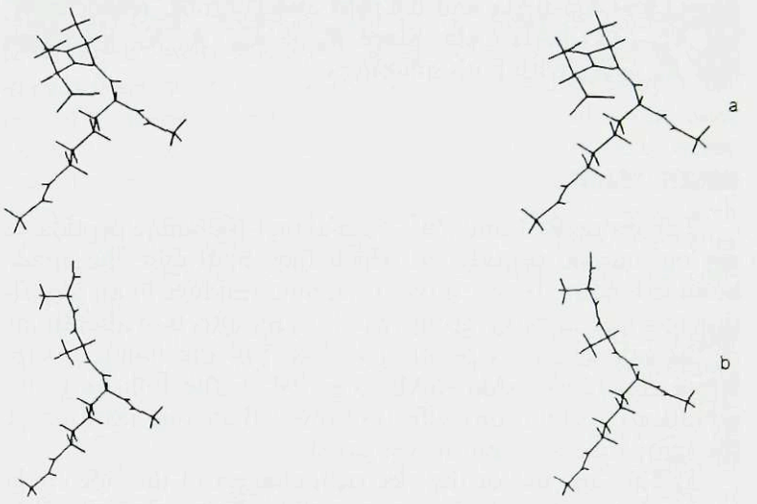


Fig. 9. *Stereoscopic diagrams of the leader conformers of* $Ac_2$-LLys-LAla-DAla *(beb*; Fig. a) and Ac*$_2$*-LLys-DAla-LAla (bb*b; Fig. b)*

$= 0.33$ mM), the DLeu[3] or DLys[3] analogues have $K_m$ values, and the DLeu[2] or DGlu[2] analogues have $K_i$ values, that are either unchanged or at the most increased by a factor of 2.5 (in fact such variations are at the limit of the experimental errors). However, contrary to that which is observed with the R61 enzyme, modifications at position 3 (peptides 6 and 7) have little effect on the $V$ of the reactions catalysed by the G enzyme. With peptide 6, the $V$ value is decreased at the most by a factor of 3. With peptide 7, the estimated 2.4-fold increased $K_m$ value well explains the 2.8-fold decreased catalytic efficiency so that the $V$ value is probably unaltered. Similarly, the $Ac_2$-LLys-DAla-DGlu (not shown in Table 1) has a $K_m$ value of 0.7 mM and a catalytic efficiency of 3000 $M^{-1}\ s^{-1}$, also suggesting that the $V$ value is identical to that of $Ac_2$-LLys-DAla-DAla.

*Replacing DAla by Gly at Position 2 or 3 of* $Ac_2$*-LLys-DAla-DAla*

The Gly[2] and Gly[3] analogues (peptides 8 and 9 in Tables 1 and 4) encompass a larger conformational space. With the Gly[2] analogue, conformers bb*b* and eb*b* disappear and are replaced by conformers eeb* and beb* while conformer beb* becomes leader (Fig. 8a). With the Gly[3] analogue, conformer eb*b* disappears and is replaced by conformer e*b*b* while conformer ee*d becomes leader (Fig. 8b). In all cases, however, the $\Sigma P_{relative}$ (bb*b*, eb*b*, be*b* and ee*b*) values are still about 35–40%.

With the R61 enzyme and when compared to $Ac_2$-LLys-DAla-DAla, the $K_m$ value of the Gly[2] analogue is unaltered and that of the Gly[3] analogue is increased by a factor of 3. It thus follows that the 660-fold and 13-fold decreased catalytic efficiencies that are observed with the Gly[2] and Gly[3] analogues, respectively, are mainly, if not entirely, due to decreased $V$ values.

With the G enzyme and in marked contrast to that which is observed with the R61 enzyme, the $K_m$ values for the Gly[3] analogue and, to a much greater extent, the Gly[2] analogue are considerably increased (when compared to $Ac_2$-LLys-DAla-DAla) so that the observed decreased catalytic efficiencies are due mainly, if not entirely, to a loss of binding efficiency.

*Replacing DAla by LAla at Position 2 or 3 of* $Ac_2$*-LLys-DAla-DAla*

These alterations (peptides 2 and 3 in Tables 1 and 4) result in probability patterns where conformers ee*b*, bb*b*, be*b* and eb*b* are no longer present. With the LAla[2] analogue, the $\Sigma P_{relative}$ (eeb*, bbb*, beb*, ebb*) is 91.6% and the leader conformer is beb* (Fig. 9a); with the LAla[3] analogue, the $\Sigma P_{relative}$ (ee*b, bb*b, be*b, eb*b) is 78% and the leader conformer is bb*b (Fig. 9b). Note that when LAla

occurs instead of DAla at position 2 or 3 (see maps 6 and 10 and 11 and 15 in Fig. 4), the points b and b* differ from each other only by $+40°$ or $-40°$ for both $\phi$ and $\psi$ angles; however, the methyl groups are displaced from one side to the other side of the plane (compare Fig. 9b and 6b).

The LAla$^2$ and LAla$^3$ analogues are not substrates of any of the enzymes under consideration. At a 10 mM concentration, they are not recognized by the R61 enzyme and do not bind to it. Both of them, however, inhibit the hydrolysis of Ac$_2$-LLys-DAla-DAla by the G enzyme but the inhibition is clearly non-competitive, indicating that the ternary complex ESI can be formed. Binding of the LAla$^2$ and LAla$^3$ analogues to the G enzyme has little influence on the $K_m$ value of Ac$_2$-LLys-DAla-DAla, suggesting that these peptide inhibitors do not occupy the main substrate binding site (i.e. the enzyme pockets where the C-terminal DAla-DAla sequence undergoes binding; see Fig. 1). The values of $K_i$ (dissociation constant of $E + I \rightleftharpoons EI$) and $K_i'$ (dissociation constant of $ES + I \rightleftharpoons ESI$) are 0.34 mM and 1.06 mM, respectively, for Ac$_2$-LLys-LAla-DAla and 0.6 mM and 0.7 mM, respectively, for Ac$_2$-LLys-DAla-LAla. Since $K_m' = K_m \cdot K_i'/K_i$, it follows that $K_m' \approx K_m$ with both inhibitors.

## DISCUSSION

The serine R61 and $Zn^{2+}$ G D-alanyl-D-alanine peptidases act on anionic peptides in which they hydrolyse the amide bond extending between two D-alanine residues in an $\alpha$ position to a free carboxyl group. Study of the effects of alterations of the side chains at position 1, 2 or 3 of the standard substrate Ac$_2$-LLys$^1$-DAla$^2$-DAla$^3$ has led to the following observations. Alterations affecting more than one position at the same time were not investigated.

a) The size and/or the electrical charges of the side chain at position 1, 2 or 3 of LDD tripeptides have relatively little influence on the backbone conformation of the tripeptides. Indeed, among the many conformers of minimal energy of the $\phi_i\psi_i$ space that characterize Ac$_2$-LLys-DAla-DAla and the LDD tripeptide analogues that have been studied, conformers ee*b*, bb*b*, be*b* and eb*b* are the most probable ones. Although depending on the peptides, these conformers may have varying relative probability $P$ values (so that the leader conformer is not always the same), the sum of the $P$ values is always 90% or more. When compared to the LDD tripeptides, the Gly$^1$, Gly$^2$ or Gly$^3$ analogues encompass a larger conformational space but the above $\Sigma P$ values are still as high as 35–50%.

b) All the above peptides except the Gly$^2$ and Gly$^3$ analogues in the case of the $Zn^{2+}$ enzyme, bind with much the same efficacy to the active centres of either the $Zn^{2+}$ or the serine enzyme (at least within a range of variation of the $K_m$ or $K_i$ values less than one order of magnitude). Hence, side chains of varying structures and/or electrical charges at position 1, 2 or 3 that have little influence on the relative probability distribution of conformers, have also no or little influence on the binding of the peptides to the enzymes. In other studies, Virudachalam and Rao [23] have suggested that D-alanyl-D-alanine peptidase activity (and therefore binding of the substrate to the enzyme) depends on specific $\phi\psi$ angle values of the fourth and fifth residues of the pentapeptide units of the peptidoglycan; these values fall in the allowed regions as defined by the data of Tables 3 and 4. Other conclusions brought about by the present studies are that (a) as the high $K_i$ values of Ac-DAla-DAla indicate, the entire length of the tripeptide backbone (and not only its C-terminal dipeptide) is involved in the binding process; and (b) side chains having at least the size of that of DAla at position 3 and, more important, at position 2 are required for efficient binding of the tripeptide to the $Zn^{2+}$ G enzyme (but not to the serine R61 enzyme). A final observation also deserves attention which is that somehow, the dipeptide Ac-DAla-DGlu binds to the $Zn^{2+}$ and serine enzymes more effectively than the dipeptide Ac-DAla-DAla, but with the same efficacy as that of Ac$_2$-LLys-DAla-DAla.

c) Binding of a peptide to the enzymes is not always followed by catalysis. Structural features at position 1, 2 or 3 in the peptides that are compatible with efficient binding may result in low turnover numbers and, at the limit, may completely prevent catalysis, thus conferring on the modified peptides the property to behave as competitive inhibitors. With the serine enzyme, replacing DAla at position 2 (i.e. that residue whose carbonyl carbon is transferred to $H_2O$) by other D-amino acids or glycine and shortening the side chain at position 1 have such effects. Replacing DAla at position 3 (i.e. the leaving group of the reaction) by other D-amino acids or Gly markedly decrease the velocity of the reactions catalysed. The same observations apply to the $Zn^{2+}$ enzyme except that (a) replacing DAla at position 2 by Gly has its main adverse effect on the binding process (see above); and (b) replacing DAla at position 3 by other D-amino acids or Gly is compatible with high turnover numbers.

d) The main backbone of Ac$_2$-LLys-DAla-DAla has a tendency to adopt a ring-like shape from which the LLys side chain protrudes as an extended structure forming with the C-terminal DAla-DAla, an angle varying between 120° and 180° (depending on the conformers). One may hypothesize that such a disposition is important in that it probably confers on the COOH terminal group, the scissile amide bond, and the three side chains at positions 1, 2 and 3, respectively, the capacity of interacting regiospecifically and stereospecifically with the different binding and catalytic sites of the active centres of the enzymes. Binding of a peptide to the enzyme occurs in the absence of any side chain at position 1 but substrate activity does require a long side chain at this position. By interacting with the relevant pocket of the enzyme cavity (Fig. 1), the LLys side chain of Ac$_2$-LLys-DAla-DAla, whose $N^{\varepsilon}$-acetyl group is located about 1–1.5 nm from the scissile amide bond, is thought to induce conformational changes in the protein that result in the establishment of a catalytically active serine residue [4, 24]. As the kinetic data show, the interaction of the LLys side chain with the corresponding enzyme pocket does not significantly increase the efficacy of the binding step. It may be that the decrease of free energy caused by this interaction is utilized to distort the enzyme-substrate system (the enzyme, the substrate, or both) and to bring it closer to the transition state. When compared to a peptide that does not possess a long side chain at position 1, Ac$_2$-LLys-DAla-DAla would interact with the enzyme with the same binding constant but the resulting complex would be considerably different (distorted versus non-distorted).

e) In the benzylpenicillin and cephaloglycine molecules (Fig. 10), $\psi_2$ and $\phi_3$ are fixed to the indicated values (Table 5) by the lactam and the thiazolidine (dihydrothiazine) rings, while $\phi_2$ and $\psi_3$ determine the orientation of the amino-acyl substituent and that of the C-terminal grouping, respectively. The dihedral angles $\phi_3$ in cephaloglycine and $\phi_2$ in both benzylpenicillin and cephaloglycine widely differ from $\phi_3$ and $\phi_2$ in the peptides (Table 5). In addition, $\omega_2$ is 136° in benzylpenicillin, 154° in cephaloglycine and 180° in the

Table 5. *Dihedral angles of the* DAla-DAla *portion of* $Ac_2$-LLys-DAla-DAla *and of the fused ring systems of benzylpenicillin and cephaloglycine*
Results for benzylpenicillin and cephaloglycine are taken from [25,26]

| Compound | $\phi_2$ | $\psi_2$ | $\omega_2$ | $\phi_3$ | $\psi_3$ |
|---|---|---|---|---|---|
| $Ac_2$-LLys-DAla-DAla: | | | | | |
| (e or b) e*b* | 80° | −80° | 180° | 160° | 20° |
| (e or b) b*b* | 160° | −160° | 180° | 160° | 20° |
| Benzylpenicillin | −93° | −128° | 136° | 149° | 42° |
| Cephaloglycine | −138° | −120° | 154° | 36° | 55° |

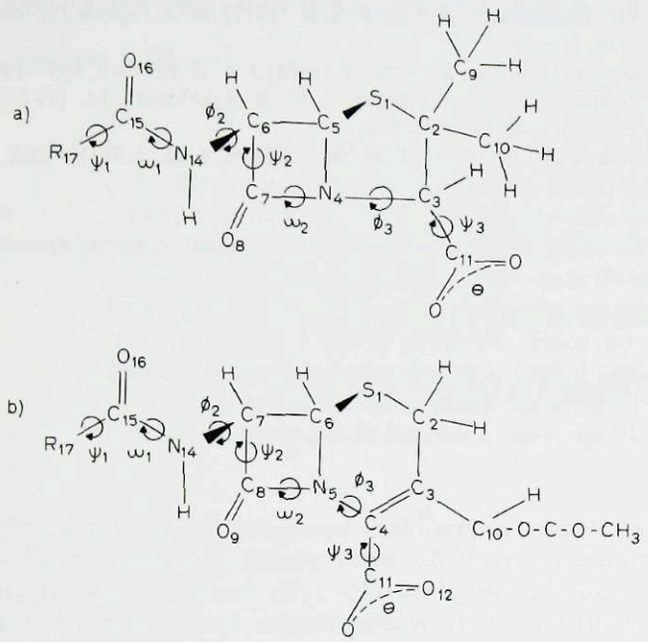

Fig. 10. *Dihedral angles around the β-lactam endocyclic amide bond in the penicillins (a) and $\Delta^3$-cephalosporins (b)*

peptides. Yet, the penicillins and $\Delta^3$-cephalosporins bind to the $Zn^{2+}$ G and serine R61 enzymes and moreover, with this latter enzyme, part of the steps involved in normal catalysis occur so that the serine residue of the enzyme centre effectively attacks the carbonyl carbon of the β-lactam amide bond to give rise to a penicilloyl-enzyme or cephalosporoyl-enzyme intermediate [4]. With the $Zn^{2+}$ enzyme, however, binding of penicillin or $\Delta^3$-cephalosporin is essentially reversible. The enzyme cavity of the $Zn^{2+}$ G and serine R61 D-alanyl-D-alanine peptidases thus appears to be able to bind LDD peptides and β-lactam antibiotics in spite of the fact that only a small portion of their conformational spaces coincide, suggesting different modes of binding for these two types of compounds. To some extent, this situation is reminiscent of that of carboxypeptidase B. In addition to its affinity toward substrates with terminal basic amino acids, carboxypeptidase B also possesses intrinsic activity against substrates with non-basic hydrophobic amino acids and the modes of binding of these two types of substrate are not the same [27].

f) Neither $Ac_2$-LLys-LAla-DAla nor $Ac_2$-LLys-DAla-LAla binds to the serine enzyme (at least at a 10 mM concentration). With the $Zn^{2+}$ enzyme, these two analogues behave as noncompetitive inhibitors. The ternary complex ESI formed between enzyme, substrate and inhibitor is non-productive. Moreover, the inhibitors exert no or little influence on the $K_m$ value of $Ac_2$-LLys-DAla-DAla, indicating that they do not occupy the site where binding of the substrate occurs. Note that peptides that are neither carbonyl donors nor amino acceptors are also known to be involved in some allosteric action on the R39 serine D-alanyl-D-alanine peptidase [28]. The most probable conformers of both $LAla^2$ and $LAla^3$ analogues differ from those of the LDD peptides. However, the $\phi_2, \psi_2$ spaces defined by conformers bbb* and ebb* of the $LAla^2$ analogues and by conformers bb*b* and eb*b* of $Ac_2$-LLys-DAla-DAla are only distant from each other by +40° or −40°. Similarly, the $\phi_3, \psi_3$ point of conformers ee*b, bb*b, be*b and eb*b of the $LAla^3$ analogue is only distant from the $\phi_3, \psi_3$ point of $Ac_2$-LLys-DAla-DAla by +40° or −40°. Hence, the inability of the $LAla^2$ and $LAla^3$ analogues to bind to the active centres of the $Zn^{2+}$ and serine enzymes might be due to a disallowed orientation of the corresponding methyl groups (which when compared with $Ac_2$-LLys-DAla-DAla are displaced from one side to the other side of the plane) as well as to a perturbed backbone conformation.

g) The conformational studies described in this paper should be useful in exploring the architecture and functioning of the active centres of the D-alanyl-D-alanine peptidases. Their full significance, however, must await completion of other studies now in progress which deal with the design of other types of enzyme inhibitors and the X-ray analysis at 0.17 nm and amino acid sequencing of the $Zn^{2+}$ G and serine R61 enzymes.

This work has been supported in part by grants (to JMG) from the Belgian Government (*Action concertée*, convention 79/84-I1), the *Fonds de la Recherche Scientifique Médicale*, Brussels, Belgium (contract 3.4501.79) and the National Institutes of Health, USA (contract 5 R01 AI-13364-05). JLDC is *chercheur qualifié* at the *Fonds National de la Recherche Scientifique*, Brussels, Belgium. HRP was in receipt of a Programme Grant from the Medical Research Council. We thank Prof. J. Toussaint (Laboratoire de Cristallographie, Université de Liège) for his interest.

## REFERENCES

1. Duez, C., Frère, J. M., Geurts, F., Ghuysen, J. M., Dierickx, L. & Delcambe, L. (1978) *Biochem. J. 175*, 793–800.
2. Frère, J. M., Ghuysen, J. M., Perkins, H. R. & Nieto, M. (1973) *Biochem. J. 135*, 463–468.
3. Frère, J. M., Moreno, R., Ghuysen, J. M., Perkins, H. R., Dierickx, L. & Delcambe, L. (1974) *Biochem. J. 143*, 233–240.
4. Ghuysen, J. M., Frère, J. M., Leyh-Bouille, M., Coyette, J., Dusart, J. & Nguyen-Distèche, M. (1979) *Annu. Rev. Biochem. 48*, 73–101.
5. Ghuysen, J. M. (1980) in *Topics in Antibiotic Chemistry* (Sammes, P.G., ed.) vol. 5, pp. 9–117, Ellis Horwood, Chichester.
6. Dideberg, O., Joris, B., Frère, J. M., Ghuysen, J. M., Weber, G., Robaye, R., Delbrouck, J. M. & Roelandts, I. (1980) *FEBS Lett. 117*, 215–218.
7. Dideberg, O., Charlier, P., Dupont, L., Vermeire, M., Frère, J. M. & Ghuysen, J. M. (1980) *FEBS Lett. 117*, 212–214.
8. Frère, J. M., Duez, C., Ghuysen, J. M. & Vandekerkhove, J. (1976) *FEBS Lett. 70*, 257–260.

9. Duez, C., Joris, B., Frère, J. M., Ghuysen, J. M. & Van Beeumen, J. (1981) *Biochem. J. 193*, 75–82.
10. Leyh-Bouille, M., Coyette, J., Ghuysen, J. M., Idczak, J., Perkins, H. R. & Nieto, M. (1971) *Biochemistry, 10*, 2163–2170.
11. Leyh-Bouille, M., Nakel, M., Frère, J. M., Johnson, K., Ghuysen, J. M., Nieto, M. & Perkins, H. R. (1972) *Biochemistry, 11*, 1290–1298.
12. Nieto, M., Perkins, H. R., Leyh-Bouille, M., Frère, J. M. & Ghuysen, J. M. (1973) *Biochem. J. 131*, 163–171.
13. Dideberg, O., Frère, J. M. & Ghuysen, J. M. (1979) *J. Mol. Biol. 129*, 677–679.
14. Knox, J. R., DeLucia, M. L., Murthy, N. S., Kelly, J. A., Moews, P. C., Frère, J. M. & Ghuysen, J. M. (1979) *J. Mol. Biol. 127*, 217–218.
15. DeLucia, M. L., Kelly, J. A., Mangion, M. M., Moews, P. C. & Knox, J. R. (1980) *Phil. Trans. R. Soc. Lond. B, 289*, 374–376.
16. Georgopapadakou, N. H., Liu, F. Y., Ryono, D. E., Neubeck, R. & Ondetti, M. A. (1981) *Eur. J. Biochem. 115*, 53–57.
17. Martin, H. H., Maskos, C. & Burger, K. (1975) *Eur. J. Biochem. 55*, 465–473.
18. Schilf, W., Frère, Ph., Frère, J. M., Martin, H. H., Ghuysen, J. M., Adriaens, P. & Meesschaert, B. (1978) *Eur. J. Biochem. 85*, 325–330.
19. Ralston, E. & De Coen, J. L. (1974) *J. Mol. Biol. 83*, 393–420.
20. De Coen, J. L. & Ralston, E. (1977) *Biopolymers, 16*, 1929–1943.
21. Ramachandran, G. N. & Sasisekharan, V. (1968) *Adv. Protein Chem. 23*, 283–438.
22. Barnickel, G., Labischinski, H., Bradazek, H. & Giesbrecht, P. (1979) *Eur. J. Biochem. 95*, 157–165.
23. Virudachalam, R. & Rao, V. S. R. (1978) *Biopolymers, 17*, 2251–2263.
24. Nieto, M., Perkins, H. R., Leyh-Bouille, M., Frère, J. M. & Ghuysen, J. M. (1973) *Biochem. J. 131*, 163–171.
25. Virudachalam, R. & Rao, V. S. R. (1977) *Int. J. Peptide Protein Res. 10*, 51–59.
26. Dexter, D. & Van der Veen, J. (1978) *J. C. S. Perkin I*, 185–190.
27. Zisapel, N., Kurn-Abramowitz, N. & Sokolovsky, M. (1973) *Eur. J. Biochem. 35*, 507–510.
28. Perkins, H. R., Frère, J. M. & Ghuysen, J. M. (1981) *FEBS Lett. 123*, 75–78.

J.-L. De Coen, Laboratoire de Chimie Biologique, Département de Biologie, Moléculaire, Faculté des Sciences de l'Université Libre de Bruxelles, Rue des Chevaux 67, B-16040, Rhode-St.-Genèse, Belgium

J. Lamotte-Brasseur, Laboratoire de Cristallographie, Institut de Physique, Université de Liège au Sart-Tilman, 4000 Liège, Belgium

J.-M. Ghuysen and J.-M. Frère, Service de Microbiologie, Institut de Chimie, Université de Liège au Sart-Tilman, 4000 Liège, Belgium

H. R. Perkins, Department of Microbiology, Life Sciences Building, P.O. Box 147, Liverpool, Lancashire, Great Britain, L69 3BX